

Copper–Sulfur Proteins: Using Raman Spectroscopy To Predict Coordination Geometry

COLIN R. ANDREW AND JOANN SANDERS-LOEHR*

Department of Chemistry, Biochemistry, and Molecular Biology, Oregon Graduate Institute of Science and Technology, Portland, Oregon 97291-1000

Received December 30, 1995

Introduction

Of all the classes of metalloproteins, the intensely colored Cu(II)–thiolate sites of cupredoxins hold a particular fascination for chemists, in terms of both their novel spectroscopy and coordination chemistry and the extent to which this copper structure controls the flow of electrons in such fundamental processes as photosynthesis and respiration.^{1,2} The term cupredoxin was originally proposed³ as a general name for the blue copper proteins to emphasize their common origin and their role as redox mediators, analogous to the iron-containing ferredoxins. An amazing feature of cupredoxins is their ability to accommodate a variety of Cu(II) coordination geometries in both native and engineered states,⁴ and a wide range of colors are associated with these different cupric thiolate structures (Figure 1). Understanding and predicting which types of structures give rise to these different spectroscopic features is a major accomplishment of resonance Raman (RR) spectroscopy, a vibrational technique which offers outstanding structural sensitivity for the metal site environment.

Copper–Sulfur Redox Centers

The traditional classification of Cu(II) proteins as type 1, type 2, or Cu_A was based on the nature and magnitude of the EPR hyperfine coupling (Figure 1). In the case of cupredoxins, the presence of a cysteine thiolate ligand provides an additional means of copper-site classification based on S → Cu(II) charge-transfer absorption. The classic type 1 copper proteins are blue (maximum absorbance at 600 nm) with a cysteine sulfur and two histidine nitrogens providing three strong ligands in a trigonal array, as in plastocyanin and azurin.² However, other members of this class, such as nitrite reductase, are green (maximum absorbance at 460 nm) due to a displacement of the copper

toward a weak axial ligand, L, yielding a distorted tetrahedral geometry.^{2,5} Through site-directed mutagenesis, type 2 cupric cysteinate sites have been created in azurin⁶ and superoxide dismutase⁵ that contain a square planar array of ligands and are yellow in color (maximum absorbance at 400 nm). This is the most common Cu(II) coordination geometry in model compounds and in proteins lacking cysteine ligands.⁷ Finally, the evolutionarily related Cu_A centers of cytochrome *c* oxidase and nitrous oxide reductase are purple (maximum absorbance at 480 and 530 nm) due to the presence of a second Cys ligand which allows the binding of two coppers with bridging by two thiolates.⁸ The Cu_A sites are found in a mixed-valence Cu(I)–Cu(II) state where the single unpaired electron is completely delocalized over the two copper atoms.

The geometry of the copper center has important consequences for the function of cupredoxins: carrying out long-range electron transfer to redox sites in other proteins. The unusual distorted tetrahedral coordination of type 1 sites is a compromise between the preferred geometries of Cu(II) and Cu(I) ions and, thereby, helps to speed electron transfer by lowering the kinetic barrier (reorganization energy) to redox interconversion.⁹ When the geometry is changed drastically, such as in the engineered type 2 azurins where a square planar coordination favors Cu(II), the proteins lose their capacity for reversible electron transfer. In the purple Cu_A centers, the distorted tetrahedral coordination of each copper is maintained and the effective symmetry of the Cu₂S₂Im₂ cluster allows for complete electron delocalization, thereby ensuring that the small reorganization energy is extended over both copper ions.⁹ The Cu₂S₂ core more strongly limits variations in geometry, with the result that the properties of the cluster are less affected by the exact placement of the terminal ligands than in

Colin R. Andrew received a B.Sc. degree in chemistry from the University of Nottingham in 1988. He received his Ph.D. degree in 1992 from the University of Newcastle upon Tyne, studying the copper protein hemocyanin under the guidance of Professor A. G. Sykes. He has been a postdoctoral fellow at the Oregon Graduate Institute since 1992, where he has been the primary driving force for the research program described in this Account.

Joann Sanders-Loehr received a B.S. degree in biochemistry from Cornell University in 1964. Her graduate work was also performed at Cornell University, where she earned a Ph.D. degree in biochemistry in 1969 for research on the structure of alanine transfer RNA under the direction of Professors Elizabeth B. Keller and Robert W. Holley. She was first introduced to metalloproteins as a postdoctoral research fellow with Professor Howard S. Mason at the Oregon Health Sciences University. This led to her long-term collaboration with Professor Thomas M. Loehr on the application of Raman spectroscopy to the study of metalloproteins. Dr. Sanders-Loehr was a faculty member in the Department of Chemistry at Portland State University from 1971 to 1984, when she moved to her present position as Professor of Biochemistry at the Oregon Graduate Institute. Her current research focuses on the spectroscopic characterization of iron, copper, and quinone cofactors in enzymes.

- (1) Sykes, A. G. *Adv. Inorg. Chem.* **1991**, *36*, 377–408.
- (2) Adman, E. T. *Adv. Protein Chem.* **1991**, *42*, 145–197.
- (3) Adman, E. T. In *Metalloproteins*; Harrison, P., Ed.; Verlag Chemie: Weinheim, FRG, 1985; Part I, pp 1–42.
- (4) Canters, G. W.; Gilardi, G. *FEBS Lett.* **1993**, *325*, 39–48.
- (5) (a) Han, J.; Loehr, T. M.; Lu, Y.; Valentine, J. S.; Averill, B. A.; Sanders-Loehr, J. *J. Am. Chem. Soc.* **1993**, *115*, 4256–4263. (b) Lu, Y.; LaCroix, L. B.; Lowery, M. D.; Solomon, E. I.; Bender, C. J.; Peisach, J.; Roe, J. A.; Gralla, E. B.; Valentine, J. S. *J. Am. Chem. Soc.* **1993**, *115*, 5907–5918.
- (6) den Blaauwen, T.; Hoitink, C. W. G.; Canters, G. W.; Han, J.; Loehr, T. M.; Sanders-Loehr, J. *Biochemistry* **1993**, *32*, 12455–12464.
- (7) Kitajima, N. *Adv. Inorg. Chem.* **1993**, *39*, 1–77.
- (8) (a) Tsukihara, T.; Aoyama, H.; Yamashita, E.; Tomizaki, T.; Yamaguchi, H.; Shinzawa-Itoh, K.; Nakashima, R.; Yaono, R.; Yoshikawa, S. *Science* **1995**, *269*, 1069–1074. (b) Iwata, S.; Ostermeier, C.; Ludwig, B.; Michel, H. *Nature* **1995**, *376*, 660–669. (c) Wilmanns, M.; Lappalainen, P.; Kelly, M.; Sauer-Eriksson, E.; Saraste, M. *Proc. Natl. Acad. Sci. U.S.A.* **1995**, *92*, 11955–11959.
- (9) Ramirez, B. E.; Malmström, B. G.; Winkler, J. R.; Gray, H. B. *Proc. Natl. Acad. Sci. U.S.A.* **1995**, *92*, 11949–11951.

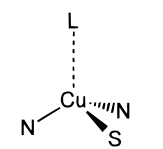
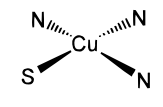
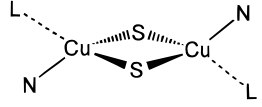
	Type 1	Type 2	Cu _A
			
Examples	Plastocyanin Azurin	Engineered Azurin Engineered SOD	Cytochrome <i>c</i> Oxidase N ₂ O Reductase
Color	Blue ↔ Green	Yellow	Purple
Absorption max. in nm	460, 600	400	480, 530, 800
EPR A _∥ in 10 ⁻⁴ cm ⁻¹	< 90 (4 lines)	> 140 (4 lines)	< 30 (7 lines)

Figure 1. Range of copper coordination geometries in copper cysteine proteins. Ligands denoted as S for cysteine thiolate, N for histidine imidazole, and L for more weakly coordinated methionine thioether or backbone carbonyl.

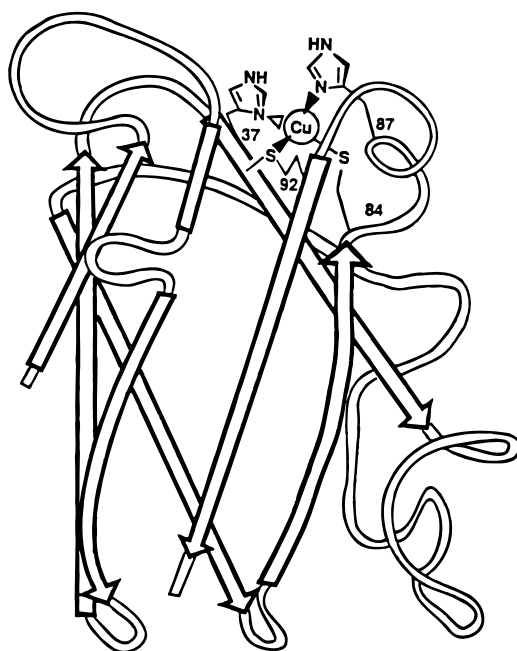


Figure 2. Structure of plastocyanin, a typical cupredoxin, with His37, Cys84, His87, and Met92 as copper ligands.¹¹

the case of mononuclear type 1 copper sites. Nevertheless, the common tetrahedral character of the mononuclear type 1 and the dinuclear Cu_A sites allows both to facilitate long-range electron transfer.

The Cupredoxin Fold

The cupredoxins are a family of evolutionarily related proteins containing an eight-stranded β -barrel or β -sandwich.^{3,10} The structure of a typical cupredoxin, plastocyanin,¹¹ is shown in Figure 2. The type 1 copper center sits close to the surface of the protein and is located between several loops from which the copper ligands derive. In native type 1 proteins, it is the protein structure which dictates the geometry of the Cu-binding site, by enforcing a rigid metal-site environment. For example, the structural integrity of the azurin metal-binding pocket is unaffected when

the copper is reduced or entirely removed.¹² Among different type 1 proteins, small changes in protein folding appear to be responsible for the variable strength of the bond to the axial ligand (generally methionine).¹³ This in turn affects the tetrahedral distortion of the site, the Cu–S(Cys) bond length, and a number of spectroscopic properties.^{13,14} In Cu_A sites, the Cu₂S₂ core is such a stable structure that there is much less scope for protein-dependent variation in coordination geometry.

Despite the rigidity of the metal-binding pocket in native proteins, its tightness can be destroyed by altering one or more of the amino acid ligands, creating a protein structure with a remarkable potential for adopting new coordination geometries. Thus, it has been possible to use genetic engineering techniques to create a range of customized Cu–S(Cys) sites.⁴ For example, replacement of the axial methionine in azurin with a stronger carboxylate ligand generates a tetrahedral site, which is referred to as type 1.5 owing to its intermediate spectroscopic properties.^{14,15} When the northern histidine ligand of azurin (analogous to His87 in plastocyanin) is replaced by the smallest amino acid, glycine, the resultant hole can be filled by external ligands. Bidentate chelators such as histamine (with imidazole and NH₂ as ligands) appear to bind *in the same plane* as the remaining Cys and His ligands, resulting in a tetragonal type 2 site with four strong ligands.⁶ An even more striking change occurs when the Cys...His...Met ligand binding loop (84, 87, and 92 in plastocyanin) is excised from azurin or amicyanin and replaced with a loop that is 2–4 residues longer and contains the sequence Cys...Cys...His...Met. The resultant engineered proteins spontaneously bind two copper atoms to form a dithiolate-bridged Cu_A site (Figure 1) similar to that of cytochrome *c* oxidase.^{16,17}

The simplest cupredoxins are soluble, monomeric

(12) (a) Shepard, W. E. B.; Anderson, B. F.; Lewandoski, D. A.; Norris, G. E.; Baker, E. N. *J. Am. Chem. Soc.* **1990**, *112*, 7817–7819. (b) Nar, H.; Messerschmidt, A.; Huber, R.; van de Kamp, M.; Canters, G. W. *FEBS Lett.* **1992**, *306*, 119–124.

(13) Guckert, J. A.; Lowery, M. D.; Solomon, E. I. *J. Am. Chem. Soc.* **1995**, *117*, 2817–2844.

(14) Andrew, C. R.; Yeom, H.; Valentine, J. S.; Karlsson, B. G.; Bonander, N.; van Pouderooyen, G.; Canters, G. W.; Loehr, T. M.; Sanders-Loehr, J. *J. Am. Chem. Soc.* **1994**, *116*, 11489–11498.

(15) Karlsson, B. G.; Nordling, M.; Pascher, T.; Tsai, L.-C.; Sjölin, L.; Lundberg, L. G. *Protein Eng.* **1991**, *4*, 343–349.

(16) Dennison, C.; Vijgenboom, E.; de Vries, S.; van der Oost, J.; Canters, G. W. *FEBS Lett.* **1995**, *365*, 92–94.

(17) Hay, M.; Richards, J. H.; Lu, Y. *Proc. Natl. Acad. Sci. U.S.A.* **1995**, *93*, 461–464.

(10) Adman, E. T. *Nature Struct. Biol.* **1995**, *2*, 929–931.

(11) Roberts, V. A.; Freeman, H. C.; Olson, A. J.; Tainer, J. A.; Getzoff, E. D. *J. Biol. Chem.* **1991**, *266*, 13431–13441.

proteins with type 1 copper sites whose function is to catalyze long-range electron transfer over distances of 10–40 Å to redox centers in other proteins.¹ Amicyanin, for example, shuttles electrons between two soluble proteins (methylamine dehydrogenase and a cytochrome *c*) in the periplasmic space. The crystal structure of the ternary complex shows that the northern histidine of amicyanin is only 5.4 Å from the edge of the tryptophan tryptophylquinone cofactor in the dehydrogenase protein.¹⁸ A number of enzymes accomplish this same type of long-range electron transfer by having the cupredoxin moiety (cupredoxin fold) incorporated directly into their covalent structure as a separate domain. Thus, ascorbate oxidase and nitrite reductase utilize the type 1 Cu site in a cupredoxin domain to transfer electrons to a substrate binding site on a separate domain.² Subunit II of cytochrome *c* oxidase contains this same cupredoxin fold,¹⁰ but with the type 1 Cu being replaced by dinuclear Cu_A which also shuttles electrons one at a time (in this case between soluble cytochrome *c* and the heme-containing active site in subunit I).⁸ Thus, the cupredoxin fold appears to have a common and widespread occurrence in copper proteins.

Resonance Raman Spectroscopy

Raman spectroscopy measures molecular vibrations by detecting the small percentage of light which undergoes inelastic scattering when the sample is illuminated by an intense light source such as a laser.¹⁹ The energy difference between the incident beam and the Raman scattered light corresponds exactly to the frequency of a molecular vibration. A dramatic increase in the Raman signal is achieved through the phenomenon of resonance Raman (RR) scattering which occurs when the input light coincides with a charge-transfer absorption. Because only the vibrations that are associated with atoms of the chromophore are resonance enhanced, RR spectroscopy provides both a remarkable degree of sensitivity and a means of selectively probing the metal–ligand centers of proteins without interference from the peptide backbone. An important point is that Raman frequencies depend on the structure of the ground state, whereas Raman intensities depend on a change in structure of the excited state. Since we know ground state structures better than those of the excited state, changes in frequency are easier to understand than changes in intensity. By labeling individual atoms with heavy isotopes, we can identify vibrational modes on the basis of their frequency downshifts due to a mass effect. In the case of the cupredoxins, we have used this approach to identify the Cu–S stretching modes of the copper cysteinyl chromophore and have found the RR spectrum to be a sensitive indicator of Cu–S(Cys) bond length and coordination geometry.

Using RR Spectroscopy To Measure the Cu–S Bond Length

The absorption spectra of type 1 Cu sites in cupredoxins are characterized by an intense (Cys)S → Cu(II)

Table 1. Spectroscopic Properties of Mononuclear Copper Cysteinate Proteins^a

copper site	λ_{\max}	$\nu(\text{Cu–S})$ in cm^{-1}	
		ν_1	ν_c
T1 Trigonal Sites			
amicyanin	595	430	430
azurin	619	408	408
azurin-H117G(Im)	625	406	406
T1 Distorted Tetrahedral Sites			
pseudoazurin	593	397	385
nitrite reductase	458	361	361
T1.5 Tetrahedral Sites			
azurin-Met121Glu	417	343	
azurin-Met121His	439	349	
T2 Tetragonal Sites			
azurin-H117G(His)	400	319	
Cu ₂ Zn ₂ SOD-His46Cys	379	342	

^a Spectroscopic data for absorption (λ_{\max} in nm) and the resonance Raman Cu–S stretch (ν_1 = frequency of most intense peak, ν_c = frequency of fundamental that generates combination bands) from ref 14, except those for azurin-Met121His which are from ref 33.

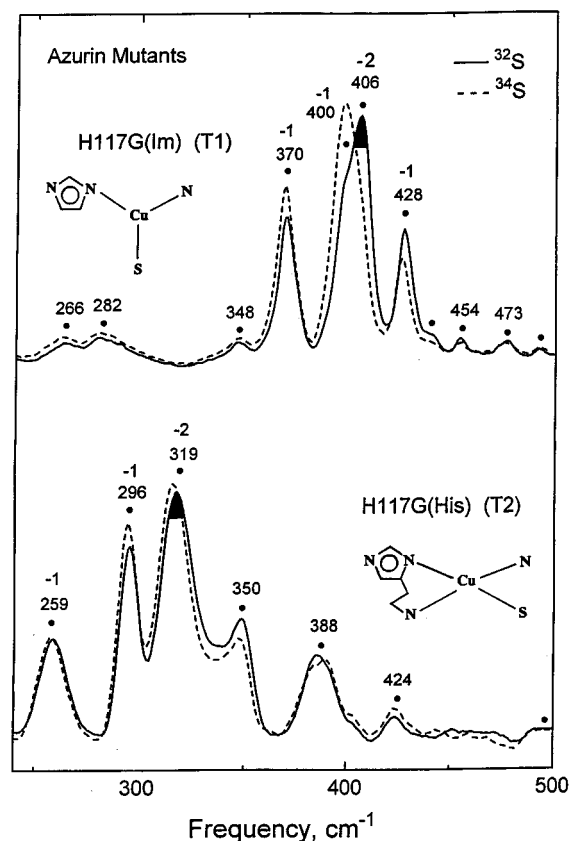


Figure 3. Resonance Raman spectra of azurin-H117G substituted with ³²S (—) or ³⁴S (---): (upper spectra) imidazole adduct probed with 647 nm excitation; (lower spectra) histidine adduct probed with 413 nm excitation. Peak frequencies are for ³²S samples with ³⁴S shifts indicated above.¹⁴

charge-transfer band near 600 nm (Table 1). For the azurin-H117G mutant in which the His 117 ligand has been replaced by Gly, addition of exogenous imidazole regenerates a type 1 Cu site with an absorption maximum at 625 nm.⁶ Excitation within this absorption band leads to a RR spectrum that is essentially identical to that of wild-type azurin with a surprisingly rich array of ~10 vibrational modes (Figure 3, upper spectra), when only a single Cu–S(Cys) stretch would have been expected to be resonance enhanced. The

(18) Chen, L.; Durley, R. C.; Mathews, F. S.; Davidson, V. L. *Science* **1994**, *264*, 86–90.

(19) Carey, P. R. *Biochemical Applications of Raman and Resonance Raman Spectroscopies*; Academic Press: New York, 1982.

key to understanding the similarly complex RR spectra of all cupredoxins has come from the use of S isotopes.^{14,20} For example, when azurin-H117G is obtained from bacteria grown on [³⁴S]sulfate, its most intense RR feature at 406 cm⁻¹ undergoes a S-isotope shift of -2 cm⁻¹, whereas the less intense peaks at 370, 400, and 428 cm⁻¹ exhibit smaller S-isotope shifts of only -1 cm⁻¹ (Figure 3, upper spectra). The multiplicity of ³⁴S-dependent modes can be ascribed to *kinematic coupling* of the Cu-S stretch with cysteine-ligand deformations (such as the S-C-C bend),²¹ a phenomenon enhanced by the coplanar conformation of the Cu-cysteinate moiety.^{22,23} The other RR modes, which lack S-isotope dependence but also appear to be cysteine-ligand deformations (see Figure 8),²⁴ presumably arise by *vibronic coupling*, a mechanism which requires that the entire cysteine ligand undergo a change in electron distribution in the electronic excited state.

In the study of azurin-H117G(Im), the most intense fundamental in the RR spectrum was found to undergo the greatest shift upon ³⁴S-substitution.¹⁴ Similar results have been obtained for wild-type azurin²⁰ and plastocyanin²⁵ where the most intense RR modes at 408 and 420 cm⁻¹, respectively, exhibit the largest S-isotope shifts of -4 and -2 cm⁻¹, respectively. Thus, the strongest feature in the RR spectrum of these proteins appears to have the most Cu-S(Cys) stretching character. This correlation is further supported by an analysis of the higher energy combination bands that result from the sum of copper cysteinate fundamentals in the 250–500 cm⁻¹ region and are ubiquitously observed for type 1 copper sites. A remarkable aspect of these bands is that they are mainly generated by a *single fundamental*, ν_c . In azurin-H117G(Im), for example, the 406 cm⁻¹ fundamental combines with the 370, 400, and 428 cm⁻¹ fundamentals to generate bands at 774, 806, and 833 cm⁻¹, respectively.¹⁴ Since ν_c generally corresponds to the most intense fundamental (Table 1), this provides another piece of evidence that the most intense band in the RR spectrum has the greatest Cu-S(Cys) stretching character.

Armed with the ability to identify $\nu(\text{Cu-S})$ from (i) its large S-isotope shift, (ii) its high RR intensity, and (iii) its role as the generator of high-frequency combination bands, we can now measure changes in the stretching frequency between different proteins and quantify this in terms of the Cu-S bond length. For example, the azurin-H117G mutant forms a yellow, type 2 adduct (λ_{max} at 400 nm) upon bidentate coordination of exogenous histidine.⁶ This species has a remarkably different RR spectrum (Figure 3, lower spectra), with its most intense peak and largest

S-isotope shift at 319 cm⁻¹, about 100 cm⁻¹ lower than that of the type 1 H117G(Im) adduct and indicative of a substantial lengthening of the Cu-S(Cys) bond. We have estimated the change in bond length using Badger's rule²⁶ and assuming a Cu-S bond length of 2.13 Å for wild-type azurin¹⁴ (the anomalously short value being typical of type 1 copper sites). A weighted average based on the S-isotope dependence yields a $\nu(\text{Cu-S})$ value of 414 cm⁻¹ for wild-type azurin and 298 cm⁻¹ for azurin-H117G(His). This 116 cm⁻¹ decrease in vibrational energy corresponds to a 0.16 Å increase in bond distance and yields an estimated Cu-S bond length of ~2.29 Å in azurin-H117G(His).¹⁴ Such a value is well within the range of Cu-S bond distances observed for tetragonal type 2 Cu sites in model compounds.²⁷

A comparison of RR spectra for a number of cupredoxins reveals a similar overall pattern of Cu-cysteinate frequencies, but with a difference in the location of the most intense bands (Table 1).²³ This variation in the clustering of intense Raman bands is a consequence of small changes in Cu-S bond length, which causes the Cu-S stretch to couple more favorably with Cys ligand deformations of different energy.¹⁴ The ability to detect $\nu(\text{Cu-S})$ shifts of only a few wavenumbers (corresponding to changes in Cu-S bond length of <0.01 Å) illustrates that the structural sensitivity of RR spectroscopy is even greater than that of X-ray crystallography.²⁸

Prediction of Coordination Geometry

Type 1 Sites. The cupredoxin protein matrix has the unique ability to stabilize a succession of Cu(II) geometries (Figure 4), each with its own characteristic spectroscopic features. As a class, type 1 copper sites are recognized by their ~600 nm absorption band, assigned to cysteinate S(π) → Cu(II) charge transfer (CT),^{13,29} and their unusually narrow EPR hyperfine coupling ($A_{\parallel} < 90 \times 10^{-4}$ cm⁻¹).³ Type 1 copper sites can be further subdivided into T1 trigonal and T1 distorted tetrahedral categories (Figure 4) on the basis of optical, EPR, and RR spectroscopy^{5,14} as well as X-ray crystallography.² In *T1 trigonal sites*, the Cu lies close to or within the planar His₂Cys array with a long (>2.8 Å) bond to the axial methionine ligand, a geometry characterized by an axial EPR spectrum and an intense blue color arising from a dominant absorption near 600 nm. The extremely short Cu-S(Cys) bond of ~2.12 Å is a consequence of having only three strong ligands and is recognized by the high energy of the $\nu(\text{Cu-S})$ mode at 405–430 cm⁻¹ (Table 1, Figure 4). In *T1 distorted tetrahedral sites*, the Cu has moved out of the His₂Cys plane with a stronger (2.6–2.8 Å) bond to the axial methionine as observed by X-ray crystallography³⁰ and contact shifts in NMR spectra.³¹ This geometry is characterized by a rhombic EPR

(20) Dave, B. C.; Germanas, J. P.; Czernuszewicz, R. S. *J. Am. Chem. Soc.* **1993**, *115*, 12175–12176.

(21) Qiu, D.; Kilpatrick, L.; Kitajima, N.; Spiro, T. G. *J. Am. Chem. Soc.* **1994**, *116*, 2585–2590.

(22) (a) Nestor, L.; Larrabee, J. A.; Woolery, G.; Reinhammar, B.; Spiro, T. G. *Biochemistry* **1984**, *23*, 1084–1093. (b) Blair, D. F.; Campbell, G. W.; Schoonover, J. R.; Chan, S. I.; Gray, H. B.; Malmström, B. G.; Pecht, I.; Swanson, B. I.; Woodruff, W. H.; Cho, W. K.; English, A. M.; Fry, A. F.; Lum, V.; Norton, K. A. *J. Am. Chem. Soc.* **1985**, *107*, 5755–5766.

(23) Han, J.; Adman, E. T.; Beppu, T.; Codd, R.; Freeman, H. C.; Huq, L.; Loehr, T. M.; Sanders-Loehr, J. *Biochemistry* **1991**, *30*, 10904–10913.

(24) Sanders-Loehr, J. In *Bioinorganic Chemistry of Copper*; Karlin, K. D., Tyeklár, Z., Eds.; Chapman & Hall: New York, 1993; pp 51–63.

(25) Qiu, D.; Dong, S.; Ybe, J. A.; Hecht, M. H.; Spiro, T. G. *J. Am. Chem. Soc.* **1995**, *117*, 6443–6446.

(26) Herschbach, D. R.; Laurie, V. W. *J. Chem. Phys.* **1961**, *35*, 458–463.

(27) Kitajima, N. *Adv. Inorg. Chem.* **1993**, *39*, 1–77.

(28) Guss, J. M.; Bartunik, H. D.; Freeman, H. C. *Acta Crystallogr., B* **1992**, *48*, 790–811.

(29) Solomon, E. I.; Baldwin, M. J.; Lowery, M. D. *Chem. Rev.* **1992**, *92*, 521–542.

(30) Murphy, M. E. P.; Turley, S.; Kukimoto, M.; Nishiyama, M.; Horinouchi, S.; Sasaki, H.; Tanokura, M.; Adman, E. T. *Biochemistry* **1995**, *34*, 12107–12117.

(31) Kalverda, A. P.; Salgado, J.; Dennison, C.; Canters, G. W. *Biochemistry* **1996**, *35*, 3085–3092.

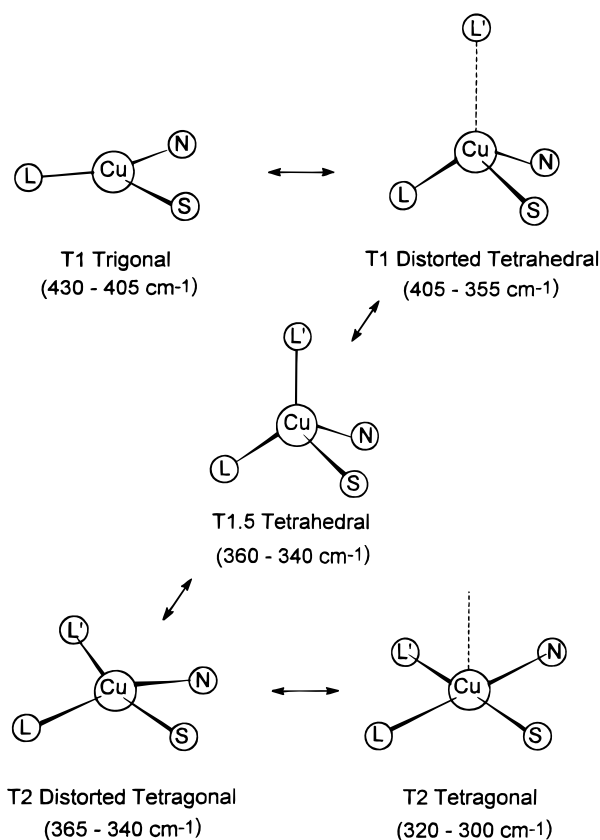


Figure 4. Detailed coordination geometries in mononuclear copper cysteinate proteins. Ligand movements required for interconversion between different geometries are shown by arrows, and the range of RR frequencies for the Cu–S(Cys) stretch is given in parentheses.

spectrum and an increased absorption at 460 nm, probably due to cysteinate $S(o) \rightarrow Cu(II)$ charge transfer.⁵ The increased interaction of the Cu with a fourth (axial) ligand in these tetrahedrally distorted sites results in a lengthening of the Cu–S(Cys) bond, as evidenced by the predominant $\nu(Cu-S)$ mode decreasing to 355–405 cm^{-1} in the RR spectrum (Table 1, Figure 4).

The T1 trigonal and T1 distorted tetrahedral sites actually represent a continuum of structures that can be distinguished by their absorption as well as their RR spectra. Pseudoazurin and nitrite reductase are both classified as distorted T1 sites on the basis of their significant absorbance near 460 nm (Figure 5). However, the site in nitrite reductase is considerably more tetrahedral according to its Cu–S(Met) bond length of 2.63 Å compared to 2.76 Å in pseudoazurin^{30,32} and Cu–S(Cys) stretching frequency of 361 cm^{-1} compared to 397 cm^{-1} in pseudoazurin. In the excitation profile for the $\nu(Cu-S)$ mode in each of these proteins, the RR intensity tracks the 460 and 600 nm absorption bands (Figure 5), demonstrating that both bands have significant (Cys)S $\rightarrow Cu(II)$ CT character.⁵ The increased absorbance at ~460 nm together with decreased absorbance at ~600 nm for nitrite reductase (Figure 5) provides another indication that it has a more tetrahedral geometry than pseudoazurin.⁵ Furthermore, an excellent correlation is obtained when the absorbance ratio ($\log(\epsilon_{460}/\epsilon_{600})$) is plotted versus the Cu–S(Cys) stretching frequency for a number of T1

Cu proteins (Figure 6). Thus, the T1 sites with trigonal planar coordination (e.g., plastocyanin and amicyanin) have the shortest Cu–S(Cys) bonds, highest RR frequencies, and minimal absorbance at 460 nm. As the sites become more tetrahedral (going toward nitrite reductase), they exhibit longer Cu–S(Cys) bonds, lower RR frequencies, and increased absorbance at 460 relative to 600 nm. Thus, the combination of optical and RR spectroscopy provides a sensitive indicator of the extent of tetrahedral distortion in T1 sites.

The sensitivity of the cupredoxin RR spectrum to changes in coordination geometry highlights an important point: the frequency of $\nu(Cu-S)$ relates to the total number of Cu ligands and their ability to donate electron density to the Cu ion. Thus, the highest $\nu(Cu-S)$ frequencies (strongest Cu–S bonds) occur in axial type 1 sites since they have only three strong ligands donating electrons to the Cu. The decrease in $\nu(Cu-S)$ frequency (and Cu–S bond strength) with tetrahedral distortion is explained by a progressive increase in the interaction with a fourth (axial) ligand. A notable deviation from the correlation of $\nu(Cu-S)$ with $\log(\epsilon_{460}/\epsilon_{600})$ occurs in the case of azurin, which has an observed $\nu(Cu-S)$ value significantly lower than predicted by its absorbance ratio. However, the apparent discrepancy of azurin is explained²⁵ by its additional weak ligand interaction from an axial C=O and its additional hydrogen bond to the S(Cys) ligand,² both of which are likely to decrease the Cu–S(Cys) bond strength without disrupting the trigonal planar character of the site.

Type 1.5 Sites. Whereas the structural continuum within the type 1 category occurs for a conserved set of ligands (2 His, 1 Cys, 1 Met) and thus is due only to variations in protein folding forces in different cupredoxins, addition of a fourth strong ligand through genetic manipulation causes more dramatic rearrangements into type 1.5 or type 2 structures. A *T1.5 tetrahedral site* (Figure 4) has been generated in azurin by replacing the Met121 ligand with a more strongly coordinating residue such as deprotonated His, Glu, or Lys.^{14,33} The crystal structure of the Met121His mutant reveals that the axial His does indeed coordinate to the Cu, creating a nearly tetrahedral site with the Cu located 0.60 Å out of the His₂Cys ligand plane and a Cu–N distance of 2.22 Å to the axial His121.³³ The spectroscopic properties of the T1.5 site lie between those of T1 and T2 sites: absorption maxima of 410–440 nm, EPR hyperfine splitting of $(90-130) \times 10^{-4} cm^{-1}$, and $\nu(Cu-S)$ values of 340–360 cm^{-1} (Table 1) resulting from the presence of a fourth strong ligand.

Type 2 Sites. The presence of four strong ligands can lead, alternatively, to a more flattened type 2 geometry with a yellow color ($\lambda_{max} < 400 nm$) and broad EPR hyperfine coupling ($A_{||} > 140 \times 10^{-4} cm^{-1}$) similar to the tetragonal copper sites of model compounds.²⁷ Raman spectra indicate that such type 2 sites can be further subdivided into two distinct categories. In *T2 tetragonal sites* (Figure 4), the very low $\nu(Cu-S)$ frequencies of 300–320 cm^{-1} indicate that the presence of a *trans ligand* directly opposite the cysteinate sulfur causes a significant lengthening

(32) Petratos, H.; Dauter, Z.; Wilson, K. S. *Acta Crystallogr., B* **1988**, *44*, 628–636.

(33) Kroes, S.; Hoitink, C. W. G.; Messerschmidt, A.; Andrew, C. R.; Ai, J. A.; Sanders-Loehr, J.; Canters, G. W. *Eur. J. Biochem.*, in press.

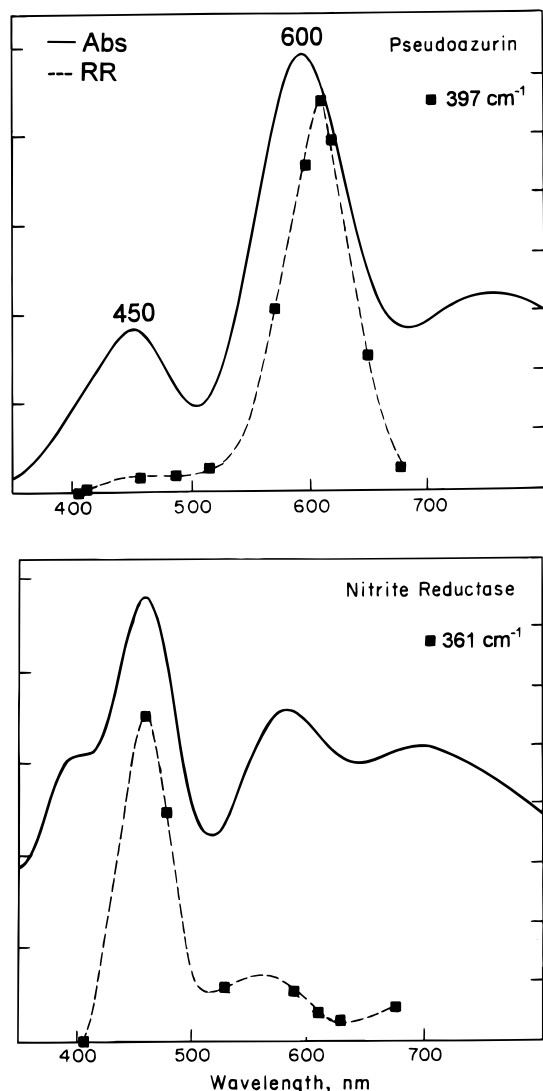


Figure 5. Absorption spectra of pseudoazurin and nitrite reductase (—) and excitation profiles for $\nu(\text{Cu-S})$ modes at 397 and 361 cm^{-1} , respectively (---). RR intensities were measured as a function of excitation wavelength using an ice mode as an internal standard.^{5a}

of the Cu-S(Cys) bond. On this basis we concluded that the histidine adduct of azurin-H117G with its $\nu(\text{Cu-S})$ at 319 cm^{-1} (Figure 3) has four strong ligands in a square planar array.¹⁴ The type 2 sites with increased $\nu(\text{Cu-S})$ values of 340–365 cm^{-1} are assigned as *T2 distorted tetragonal sites* (Figure 4) assuming there is no longer a trans ligand in the same plane as the cysteinyl sulfur. An example is the superoxide dismutase mutant with a Cys in place of the His 46 ligand in its tetragonal copper site³⁴ and its $\nu(\text{Cu-S})$ at 342 cm^{-1} (Table 1). Finally, the overlap of vibrational frequencies for the distorted tetrahedral (T1), tetrahedral (T1.5), and distorted tetragonal (T2) structures suggests that they have similar Cu-S(Cys) bond lengths and that the marked differences in their optical and EPR properties are rather a consequence of their different coordination geometries.

Purple Cu_A : A New Class of Cupredoxin Containing a Second Cys Ligand

The purple Cu_A site of cytochrome *c* oxidase provides a prime example of the ability of cupredoxins to alter

(34) Lu, Y.; Gralla, E. B.; Roe, J. A.; Valentine, J. S. *J. Am. Chem. Soc.* **1992**, *114*, 3560–3562.

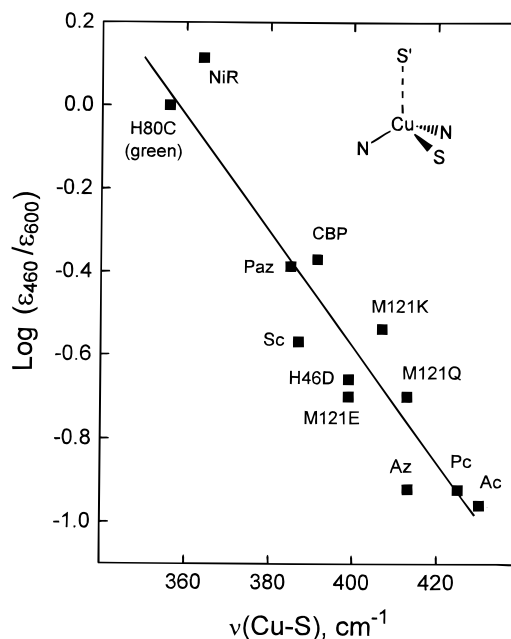


Figure 6. Correlation of the absorbance ratio (ϵ at ~ 460 nm/ ϵ at ~ 600 nm) with the Cu-S(Cys) stretching frequency for type 1 Cu sites. Proteins included are amicyanin (Ac), azurin mutants (H46D, M121E, M121K, M121Q), cucumber basic protein (CBP), nitrite reductase (NiR), pseudoazurin (Paz), plastocyanin (Pc), stellacyanin (Sc), and SOD mutant (H80C).¹⁴

their copper coordination geometry in response to a change in ligands. As the three recent crystal structures show, the Cu_A site consists of two Cu ions 2.5 Å apart, each with a terminal histidine ligand and two cysteine thiolate bridges (Figure 1).⁸ The spectroscopic comparison of Cu_A -containing proteins has revealed a remarkable conservation of the copper-site structure in (i) the cytochrome *c* oxidases from three different organisms (soluble fragments produced by gene cleavage),^{35,36} (ii) the engineered Cu_A sites of azurin,¹⁷ amicyanin,¹⁶ and purple Cytochrome A (an altered quinol oxidase),^{8c,37} and (iii) nitrous oxide reductase (another cupredoxin-domain-containing enzyme).³⁸ Each of these proteins has a purple color arising from the three absorption bands at ~ 480 , 530, and 780 nm and a seven-line EPR spectrum³⁸ characteristic of a mixed valence, $\text{Cu}(1.5)\text{-Cu}(1.5)$ redox state. There is now great interest in understanding the chemistry of these dinuclear copper sites. Key questions relate to the influence of the novel cysteine thiolate bridging geometry, the possibility of a direct Cu-Cu interaction,³⁹ and their respective roles in generating the unusually short Cu-Cu distance as well as the complete electron delocalization.

Raman spectroscopy provides the most compelling evidence for the same copper-site geometry being present in all of the above-mentioned Cu_A -containing proteins.^{35,36} As shown in Figure 7, the Cu_A moieties in cytochrome *c* oxidase (CCO), engineered azurin, and

(35) Andrew, C. R.; Han, J.; de Vries, S.; van der Oost, J.; Averill, B. A.; Loehr, T. M.; Sanders-Loehr, J. *J. Am. Chem. Soc.* **1994**, *116*, 10805–10806.

(36) Andrew, C. R.; Lappalainen, P.; Saraste, M.; Hay, M. T.; Lu, Y.; Dennison, C.; Canters, G. W.; Fee, J. A.; Slutter, C. E.; Nakamura, N.; Sanders-Loehr, J. *J. Am. Chem. Soc.* **1995**, *117*, 10759–10760.

(37) Andrew, C. R.; Nakamura, N.; Sanders-Loehr, J.; Saraste, M. Unpublished results.

(38) Antholine, W. E.; Kastrau, D. H. W.; Steffens, G. C. M.; Buse, G.; Zumft, W. G.; Kroneck, P. M. H. *Eur. J. Biochem.* **1992**, *209*, 875–881.

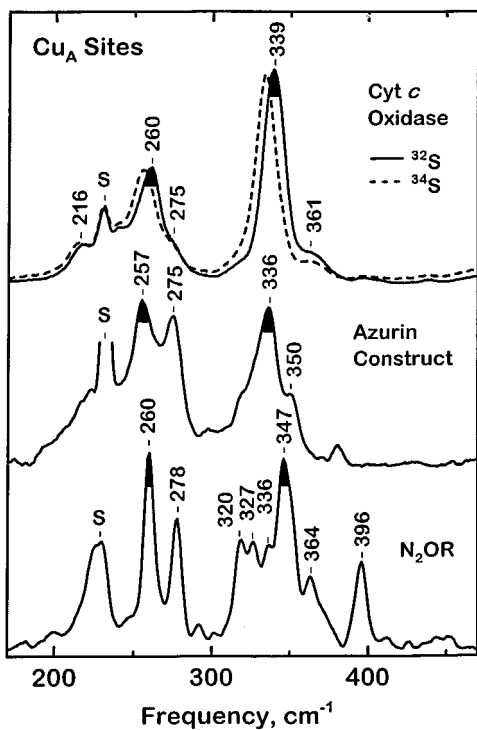


Figure 7. RR spectra of Cu_A sites obtained with 488 nm excitation: (upper trace) *Paracoccus denitrificans* cytochrome *c* oxidase fragment from bacteria grown on ^{32}S - (—) or ^{34}S -sulfate (---);³⁶ (middle trace) *Pseudomonas aeruginosa* azurin construct containing the Cu_A loop from *P. denitrificans* CCO;³⁶ (lower trace) *Achromobacter cycloclastes* nitrous oxide reductase.³⁵ S = frozen solvent.

nitrous oxide reductase (N_2OR) each exhibit the characteristic Cu_A RR signature of two intense features at 260 and 340 cm^{-1} . Their ^{34}S -isotope shifts of -4.1 and -5.1 cm^{-1} , respectively (Figure 7, upper trace), indicate that each of these vibrational modes can be assigned to a Cu–S stretching motion within the $\text{Cu}_2\text{S}_2\text{Im}_2$ core. The RR excitation profiles for CCO and N_2OR show that the same RR frequencies are observed upon excitation within the 480, 530 and 780 nm absorption bands, proving that the 260 and 340 cm^{-1} vibrations derive from the same Cu–S chromophore in both proteins.³⁵

Normal coordinate analysis has been successful in assigning the RR spectrum of the Cu_A site in CCO.⁴⁰ Both the large 80 cm^{-1} frequency separation and the large S-isotope shifts of the intense bands at 260 and 340 cm^{-1} are well fit by a dinuclear model with two bridging thiolates, thus providing the first unambiguous spectroscopic support for the structure determined by X-ray crystallography. According to this analysis, the three expected A_g symmetric stretching modes can be assigned as follows: the 340 cm^{-1} mode is the symmetric stretch of the Cu_2S_2 rhombus, the 260 cm^{-1} mode is a Cu–S stretch with substantial Cu–N(Im) contributions from the terminal histidine ligands, and the Cu-isotope sensitive mode at 140 cm^{-1} is predominantly a vibration of the two Cu atoms (Figure 9). Because this latter Cu motion could be due to either

(39) (a) Blackburn, N. J.; Barr, M. E.; Woodruff, W. H.; van der Oost, J.; de Vries, S. *Biochemistry* **1994**, *33*, 10401–10407. (b) Wallace-Williams, S. E.; James, C. A.; de Vries, S.; Saraste, M.; Lappalainen, P.; van der Oost, J.; Fabian, M.; Palmer, G.; Woodruff, W. H. *J. Am. Chem. Soc.* **1996**, *118*, 3986–3987.

(40) Andrew, C. R.; Fraczekiewicz, R.; Czernuszewicz, R. S.; Lappalainen, P.; Saraste, M.; Sanders-Loehr, J. *J. Am. Chem. Soc.*, in press.

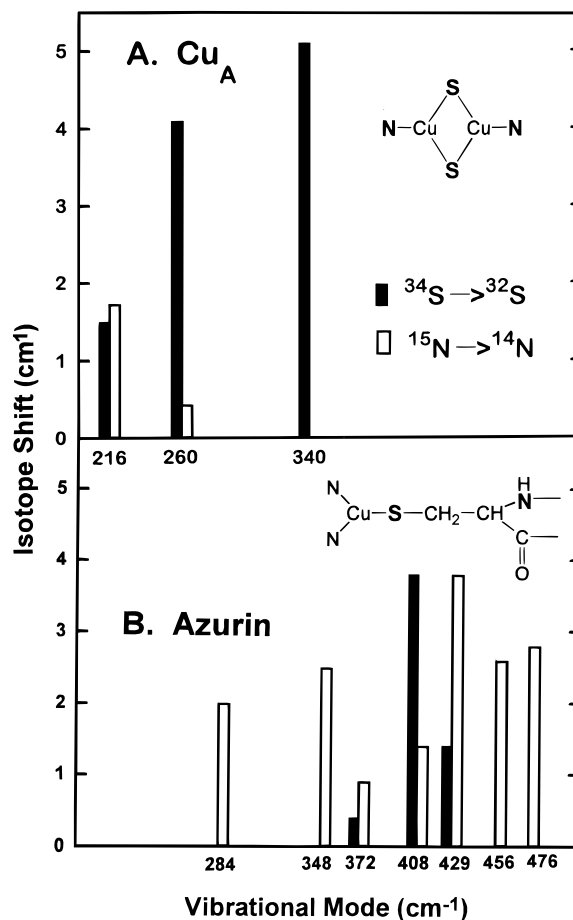


Figure 8. Sulfur and nitrogen isotope downshifts for different vibrational modes based on RR spectra for (A) Cu_A fragment from *P. denitrificans* cytochrome *c* oxidase⁴⁰ and (B) *Ps. aeruginosa* azurin.^{14,24} Cells were grown on ^{34}S -sulfate or ^{15}N -ammonia; mutant azurin prepared with ^{15}N -imidazole exhibits no significant N-isotope shifts.²⁴ Atoms in bold face are those believed to be responsible for isotope shifts.

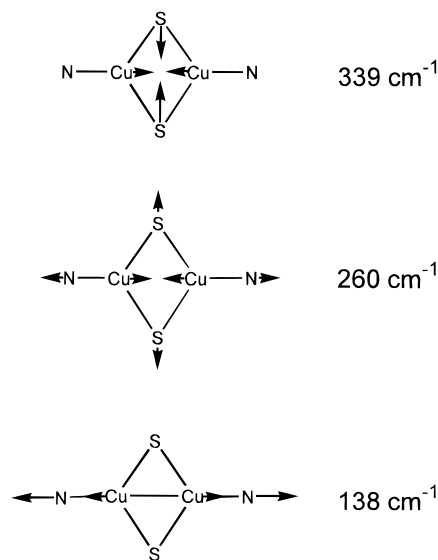


Figure 9. Calculated atomic displacements (eigenvectors) and frequencies for the three principal A_g vibrations of the Cu_A site, based on a normal coordinate analysis.⁴⁰

a Cu–S–Cu bend or a Cu–Cu stretch, RR spectroscopy cannot by itself prove or disprove the presence of a Cu–Cu bond. However, our analysis does give clear evidence that each of the Cu atoms has a distorted tetrahedral coordination geometry. The

degree of vibrational coupling between Cu–N(Im) and Cu–S stretching modes has a marked angular dependence, and the observed isotope shifts in the Cu_A site are best fit by a structure in which the Cu–N bonds of both imidazole ligands are trans-tilted by $\sim 40^\circ$ above and below the Cu₂S₂ plane.⁴⁰

There are a number of significant differences in the RR spectra of dinuclear and mononuclear Cu–cysteinate sites, and these have important structural implications. *First*, the $\nu(\text{Cu–S})$ modes at 260 and 340 cm^{-1} in the different Cu_A-containing proteins vary by only $\pm 4 \text{ cm}^{-1}$ (Figure 7) compared to a variation of $\pm 38 \text{ cm}^{-1}$ for the principal $\nu(\text{Cu–S})$ mode of type 1 cupredoxins (Figure 4). This indicates that the Cu_A site does not exhibit the continuum of structures seen for mononuclear sites. Rather, the highly conserved structure of the Cu₂S₂ core in both native Cu_A proteins and engineered constructs suggests that the short Cu–Cu distance of $\sim 2.5 \text{ \AA}$ and narrow Cu–S–Cu angle of $\sim 70^\circ$ are thermodynamically favored and less easily affected by variations in the cupredoxin fold.^{36,39} *Second*, there are marked differences in the patterns of ³⁴S dependence (Figure 8). The S-isotope shifts in cupredoxins tend to be distributed between several nearby peaks due to kinematic coupling of the Cu–S stretch with Cys modes of similar energy,^{14,20} and the total S-isotope shift in azurin is only 5 cm^{-1} . The S-isotope dependent modes in Cu_A are much more widely separated in energy, in keeping with a dithiolate bridged structure, and the total S-isotope shift of 10 cm^{-1} is considerably larger due to the contribution of two thiolate ligands. *Third*, the patterns of ¹⁵N dependence for cells grown on [¹⁵N]ammonia are also significantly different (Figure 8). Almost every RR mode in azurin has an ¹⁵N downshift of $1\text{--}4 \text{ cm}^{-1}$ due to the amide nitrogen of cysteine being involved in

ligand deformations that undergo kinematic or vibronic coupling with the copper cysteinate chromophore.²⁴ In contrast, the considerably smaller ¹⁵N downshifts of 0.5 cm^{-1} or less in Cu_A indicate that there is much less mixing with cysteinate ligand modes, allowing the RR spectrum to be effectively modeled using only a six-atom Cu₂S₂N₂ cluster.

The unique coordination geometry of the Cu₂S₂N₂ moiety in Cu_A forms spontaneously when a second cysteine ligand is introduced into the cupredoxin fold. The constancy of the vibrational frequencies in the RR spectrum (Figure 7) shows that the bond distances and bond angles in the cluster are highly conserved. The facile formation of this minimum-energy conformation explains why the same purple mixed valence state can be observed for all Cu_A sites. Despite the presence of different terminal ligands on each Cu atom (Figure 1), the symmetry of the Cu₂S₂N₂ moiety enables complete delocalization of the unpaired electron over the two Cu atoms, permitting the Cu_A site to function as a one-electron carrier. The mononuclear type 1 Cu sites in cupredoxins also function as one-electron carriers, but with a much larger range of Cu–S frequencies, indicating a range of coordination geometries between trigonal planar and tetrahedral depending on the protein environment (Figure 4). The greater stability of the dinuclear cluster toward perturbations from the protein environment could explain the driving force for the evolution of dinuclear Cu_A sites.

We thank our many collaborators who made this work possible and the National Institutes of Health for financial support (Grant GM 18865).

AR950084U